Dalton Transactions

Cite this: *Dalton Trans.*, 2012, **41**, 3780

www.rsc.org/dalton

PAPER

Metal induced folding: synthesis and conformational analysis of the lanthanide complexes of two 44-membered hydrazone macrocycles†

Jörg M. Klein,[a] Jack K. Clegg,[a] Vittorio Saggiomo,[b] Lisa Reck,[b] Ulrich Lüning*[b] and Jeremy K. M. Sanders*[a]

Received 2nd October 2011, Accepted 12th January 2012
DOI: 10.1039/c2dt11861k

Six new lanthanide complexes of two 44-membered macrocycles have been prepared and characterised in solution. An analysis of the conformations of the free macrocycles and their lanthanide complexes both in solution (2D NMR) and in solid state (X-ray crystallography) demonstrate that the complexation induces changes in folding of the macrocycles.

Introduction

The coordination chemistry of lanthanide ions has recently received increasing attention due to their potential applications in medical imaging and sensing through their magnetic and photophysical properties.[1] Owing to their large diffuse orbitals their coordination chemistry is characterised by high-coordination numbers and flexible coordination geometries.[2,3]

These features mean that the design of macrocyclic ligands capable of forming stable lanthanide complexes has remained a considerable challenge despite being a focus for more than 30 years.[3,4] Macrocyclic ligands are attractive complexing agents for lanthanides because of the many potential sizes, chelating groups and design (including solubility) features that can be incorporated into the ligand backbone.[3–5]

We have recently demonstrated that a series of large and flexible [1 + 1] and [2 + 2] macrocycles containing acylhydrazone moieties can be efficiently synthesised using a dynamic combinatorial chemistry[6] approach.[7,8] As pentadentate N_3O_2 acylhydrazone ligands[9] have been shown to be good ligands for lanthanide ions,[10–12] we investigated the complexation of lanthanide ions with two 44-membered [2 + 2] acylhydrazone containing macrocycles, the $N_{10}O_8$ **1** and the N_8O_{10} **2**. Here we report solution studies of the interaction of **1** and **2** with lanthanum(III), europium(III) and dysprosium(III) along with the X-ray structures of **1**·2MeOH, $[Eu(\mathbf{1})]_2[Eu(\mathbf{1})(H_2O)]\cdot 14H_2O\cdot 9Cl$ and $[La(\mathbf{2})(Cl)]\cdot 2Cl\cdot 1.75MeOH\cdot 7.35H_2O$.

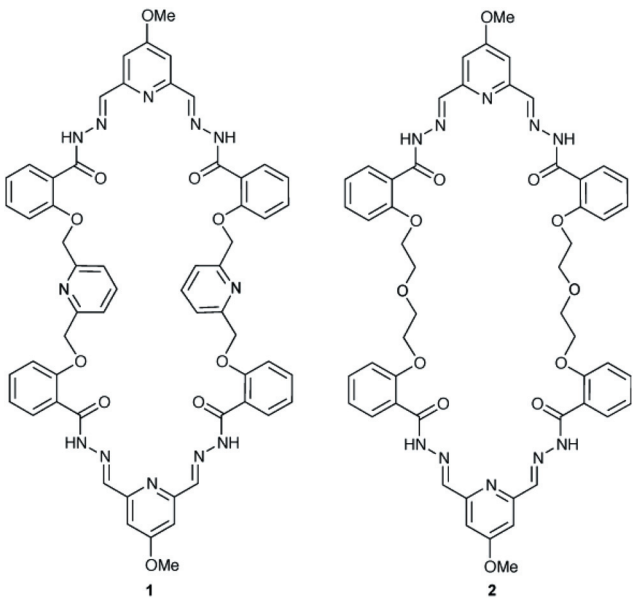

Experimental

Solvents were purchased from Romil (LC-MS grade $CHCl_3$), Fischer (HPLC grade MeOH) and Aldrich (TFA). Metal salts were purchased from Sigma-Aldrich, Lancaster, Breckland and Alpha Aesar. ^1H and ^{13}C NMR spectra were recorded on Bruker DPX-400, DRX 500, AV 600 or Advance 500 TCI Cryo Spectrometers. All signals were referenced to the solvent residue (3.31 ppm for MeOD). High-resolution (HR) electrospray ionisation (ESI) mass spectra were recorded on a Waters LCT Premier XE instrument. UV-Vis spectra were recorded in a 1 cm quartz cuvette using a Lambda 14 spectrometer from Perkin Elmer at 22 °C, unless otherwise stated. The DCLs were analysed by LCMS using an Agilent 1100 series HPLC coupled to an Agilent XCT Ion-Trap.

[a]*University Chemical Laboratory, University of Cambridge, Lensfield Road, Cambridge CB2 1EW, UK. E-mail: jkms@cam.ac.uk; Fax: +4 (0)1223 336 017*
[b]*Otto-Diels-Institut für Organische Chemie, Olshausenstr. 40, D-24098 Kiel, Germany. E-mail: luening@oc.uni-kiel.de; Fax: +49-431-880-1558; Tel: +49-431-880-2450*

†Electronic supplementary information (ESI) available: Further details of the NMR, UV-Vis and HRMS studies. CCDC reference number 847405. For ESI and crystallographic data in CIF or other electronic format see DOI: 10.1039/c2dt11861k

Solution complex studies

The macrocyclic ligands were synthesised from the corresponding dialdehyde and dihydrazide precursors as previously described.[7,8] Their lanthanide complexes were prepared by dissolving **1** (1 mM in $CHCl_3$–MeOH, 1 : 1) or **2** (in $CHCl_3$–MeOH, 7 : 3) and adding the appropriate lanthanide chloride *via* a syringe (50 mM solution in MeOH). The changes upon complexation were monitored by NMR (^{1}H and NOESY), HRMS and UV-Vis spectroscopy. No attempt was made to further purify the complexes or isolate them in the solid state due to the small quantities prepared. Crystals suitable for diffraction studies were grown by slow evaporation from MeOH–H_2O.

X-ray structures

Data were collected on a Nonius Kappa FR590 diffractometer employing graphite-monochromated Mo K_α radiation generated from a sealed tube (0.71073 Å) with ω and ψ scans at 180(2) K.[13] Data integration and reduction were undertaken with HKL Denzo and Scalepack.[14] Subsequent computations were carried out using the WinGX-32 graphical user interface.[15] Structures were solved using SIR92[16] or SUPERFLIP.[17] Multi-scan empirical absorption corrections were applied to the data set using the program SORTAV.[18] Data were refined and extended with SHELXL-97.[19] In general, non-hydrogen atoms with occupancies of greater than 0.5 were refined anisotropically, carbon-bound and nitrogen-bound hydrogen atoms were included in idealised positions and refined using a riding model. Oxygen and bound hydrogen atoms were first located in the difference Fourier map before refinement. Where these hydrogen atoms could not be located, they were not modelled. Crystallographic data and specific details pertaining to structural refinements are summarised below.

1·2MeOH

Formula $C_{60}H_{56}N_{12}O_{12}$, M 1137.17, triclinic, space group $P\bar{1}$ (#2), a = 7.7020(2), b = 13.2598(2), c = 14.3448(3) Å, α = 110.859(1), β = 100.572(1), γ = 92.073(1)°, V = 1337.50(5) Å^3, D_c = 1.412 g cm^{-3}, Z 1, crystal size: 0.28 by 0.23 by 0.12 mm, colour: light brown, habit: block, temperature: 180(2) K, λ(Mo K_α) 0.71073 Å, μ(Mo K_α) 0.101 mm^{-1}, T(SORTAV)$_{min,max}$ = 0.837, 0.901, $2\theta_{max}$ = 63.04°, hkl range: −11–11, −19–19, −21–21, N = 26330, N_{ind} = 8877 (R_{merge} = 0.0312), N_{obs} = 6651 ($I > 2\sigma(I)$), N_{var} = 384, residuals R_1(F) = 0.0493, wR_2(F^2) = 0.1344, GoF(all) = 1.020, $\Delta\rho_{min,max}$ = −0.214, 0.335 e$^-$ Å^{-3}.

[Eu(1)]$_2$[Eu(1)(H_2O)]·14H_2O·9Cl

Formula $C_{174}H_{178}Cl_9Eu_3N_{36}O_{47}$, M 4300.45, triclinic, space group $P\bar{1}$ (#2), a = 15.344(3), b = 22.768(5), c = 36.352(7) Å, α = 79.55(3), β = 87.57(3), γ = 76.21(3)°, V = 12 129(4) Å^3, D_c = 1.178 g cm^{-3}, Z = 2, crystal size: 0.07 by 0.05 by 0.02 mm, colour: yellow, habit: needle, temperature: 180(2) K, λ(Mo K_α) 0.71073 Å, μ(Mo K_α) 0.934 mm^{-1}, T(SORTAV)$_{min,max}$ = 0.938, 0.987, $2\theta_{max}$ = 34.46°, hkl range: −12–12, −18–18, −30–30, N = 25 417, N_{ind} = 13 368(R_{merge} = 0.0815), N_{obs} = 4804($I > 2\sigma(I)$), N_{var} = 1046, residuals R_1(F) = 0.0952, wR_2(F^2) = 0.3149, GoF(all) = 1.012, $\Delta\rho_{min,max}$ = −0.771, 1.326 e$^-$ Å^{-3}.

Specific refinement details. The crystals employed in this study were extremely small and poorly diffracting with reflections observed to only 1.2 Å resolution. This is in part due to considerable disorder present in the chloride anions and solvent water molecules, each of which was modelled over numerous positions. One of the methoxy methyl groups is also disordered and modelled in two equal occupancy positions. None of the water hydrogen atoms could be located and were not included in the model. Because of the limitations of the data only the europium ions were modelled anisotropically with the remaining atoms modelled isotropically. Despite the limitations with the data the structure is more than sufficient to establish chemical connectivity.

[La(2)(Cl)]·2Cl·1.75MeOH·7.35H_2O

Formula $C_{53.75}H_{71.70}Cl_3LaN_{10}O_{19.10}$, M 1408.77, monoclinic, space group $P2_1/c$ (#14), a = 16.9693(2), b = 19.9851(3), c = 20.0933(3) Å, β = 96.2340(6)°, V = 6774.01(16) Å^3, D_c = 1.381 g cm^{-3}, Z = 4, crystal size: 0.23 by 0.23 by 0.18 mm, colour: colourless, habit: block, temperature: 180(2) K, λ(Mo K_α) = 0.71073 Å, μ(Mo K_α) = 0.822 mm^{-1}, T(SORTAV)$_{min,max}$ = 0.716, 0.839, $2\theta_{max}$ = 54.98°, hkl range −21–21, −25–25, −26–25, N = 60 956, N_{ind} = 15 097(R_{merge} = 0.0503), N_{obs} = 12 368($I > 2\sigma(I)$), N_{var} = 845, residuals R_1(F) = 0.0674, wR_2(F^2) = 0.1863, GoF(all) = 1.163, $\Delta\rho_{min,max}$ = −0.990, 1.556 e$^-$ Å^{-3}.

Specific refinement details. The solvent is disordered. The methanol solvent molecules were modelled over three positions with a total occupancy of 1.75 while the water molecules were modelled over 15 positions (two full occupancy). The water hydrogen atoms could not be located in the difference Fourier map and were not modelled.

Results and discussion

Ligand structures

The [2 + 2] macrocycles **1** and **2** were synthesised by precipitation as pure solids from dynamic combinatorial libraries of the constituent dialdehyde and dihydrazide precursors as previously reported.[7,8] Both macrocycles are insoluble in water and $CHCl_3$, sparingly soluble in DMSO, MeOH and MeOH–H_2O mixtures, but are readily soluble in 50 : 50 (v : v) $CHCl_3$: MeOH mixtures. Crystals of **1**·2MeOH suitable for diffraction studies were grown by the slow evaporation of MeOH–H_2O (Fig. 1). The macrocycle crystallises about an inversion centre such that there is half of a molecule in the asymmetric unit; it adopts an S-shaped configuration with the two pyridyl-dihydrazide moieties in planar arrangements, stacking above one another.

There is a separation of ~3.4 Å between each of the acylhydrazone planes suggesting the presence of π–π interactions between layers.[20] This planar arrangement is further stabilised by the presence of both formal and informal hydrogen bonds. Each of the hydrazide protons interacts with both ether and pyridyl groups, while there is also a number of $CH_{phenylene}$–O_{ether} and

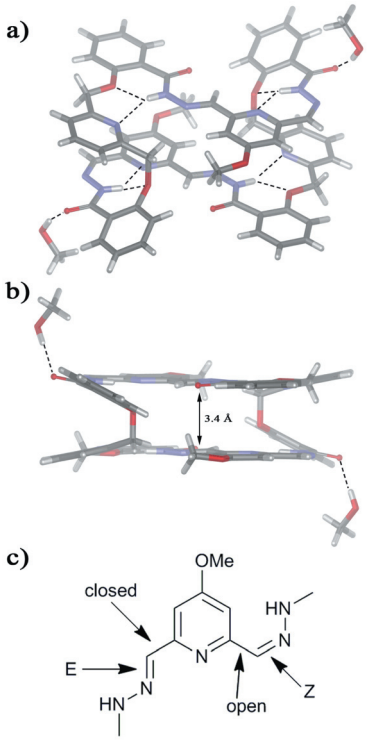

Fig. 1 (a) Top view and (b) side view of the X-ray structure of **1**·2MeOH. Dashed lines indicate hydrogen bonds.

$CH_{phenylene}$–O_{amide} interactions. The methanol solvate molecules also hydrogen bond to the amide oxygens. Adjacent molecules in the lattice interact through similar weak π–π and informal $CH_{phenylene}$–O_{ether} and $CH_{phenylene}$–N hydrogen bonds resulting in the formation of an infinite 3D lattice. The ligand's conformation contrasts with that observed in the structure of **1**·1.5H_2O·4$CHCl_3$ where a highly-twisted chiral arrangement was present.[7]

Part of the difference can be attributed to the conformation of the pyridyl-hydrazone groups. In the previously reported example, three of the four hydrazone groups were arranged in an 'open' conformation with respect to the pyridyl nitrogen such that they were not preorganised for metal binding, a structure consistent with 2D NMR solution investigations[7] and the X-ray structure of two related acyl-hydrazone ligands.[11,21] In the present structure, however, each acyl-hydrazone group is arranged in an 'open-closed' conformation (which has previously been observed in non-macrocyclic acyl-hydrazone ligands)[22] resulting in the S-shape. The hydrogen bonds discussed above stabilise these conformations. The 'open-closed' arrangement observed in the X-ray structure of **1**·2MeOH contrasts with the conformation of the structure observed in the solid state of **2**·MeOH in which there are three 'open' and one 'closed' hydrazone groups.[8] Notably, while the X-ray structure of **1**·2MeOH displays a different conformation to that observed in solution, the arrangements of **2**·MeOH are the same as observed by NMR and diffraction studies. This suggests that the pyridiyl and ethylene glycol linking units in **1** and **2**, respectively, play a significant role in the conformation and hence preorganisation of the macrocycles for metal binding. These

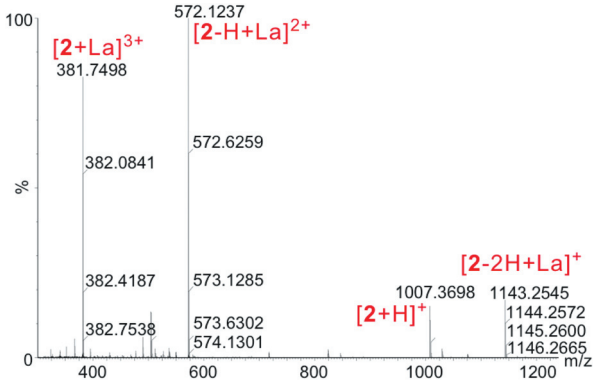

Fig. 2 (−)ESI-HRMS of $[La(\mathbf{2})]^{3+}$ in MeOD–$CDCl_3$ (1 : 1).

differences presumably arise through the different numbers of possible degrees of freedom and hence the flexibility of the linking units.

Metal complexes

The interaction of **1** and **2** with lanthanum(III), europium(III) and dysprosium(III) were investigated in solution. Samples were prepared by dissolving each of the ligands in mixtures of $CDCl_3$–MeOD (1 mM) and adding 1.0 eq. of the $LnCl_3$ (Ln = La, Eu, Dy) in MeOD (50 mM). HRMS (Fig. 2 and ESI†) showed the singly, doubly and triply charged molecular ion peaks of the complexes. Addition of excess lanthanide salts did not result in the formation of additional peaks, suggesting that only 1 : 1 complexes were formed. To further investigate the solution behaviour and confirm 1 : 1 binding, UV-Vis titrations with **1**–**2** and three different lanthanides (La^{3+}, Eu^{3+} and Dy^{3+}) were performed (Fig. 3 and ESI†).

In each case the binding isotherms indicated 1 : 1 M : L ratios with very strong binding. Fitting a published model[23] for 1 : 1 binding indicated that binding constants were larger than 10^6 M^{-1} for all the complexes investigated (Fig. 3 and ESI†).

The solution behaviour of the La^{3+} complexes of **1** and **2** were also investigated by NMR (Fig. 4 and ESI†). Comparison of the spectra of the complexed and free macrocycles showed large shifts for the imine protons (*e*) and the aromatic protons adjacent to the amide group (*h*) suggesting an involvement of the hydrazone moiety in complexation. No further change was observed in the spectra after the addition of excess lanthanide salt. The NOESY spectra of the La^{3+} complexes (ESI†) showed cross-peaks between the *meta*-pyridine protons *c* and the imine protons *e* which were not present in the NOESY spectra of the metal-free macrocycle **1**.[7,8] The NOESY spectra of metal-free **2**, however, showed a cross-peak between *c* and *e* suggesting that the metal complexation induced significant conformational changes in **1** whereas **2** appeared to be more preorganised.

Solid state structures

While each of the complexes described above for solution studies were prepared *in situ* and on a scale too small for microanalysis, in two cases slow evaporation of MeOH–H_2O solutions

of $EuCl_3$/**1** and $LaCl_3$/**2** resulted in the formation of crystals suitable for X-ray studies.

The crystal structure of the Eu^{3+} complex shows three different coordination environments in one single crystal: one in which Eu^{3+} is 9 coordinate (Fig. 5a) and two where it is 10 coordinate (Fig. 5b).

In the 9-coordinate complex the macrocycle folds such that the two N_3O_2 ends are stacked. The Eu^{3+} guest is found slightly above (0.59 Å) the plane of the 'lower' N_3O_2 motif, similar to the other crystal structure of Eu^{3+}–N_3O_2-acyl hydrazone complexes.[11,12] The remaining coordination sites are occupied by a carbonyl oxygen from the same molecule and three solvent molecules (H_2O).

In the 10-coordinate Eu^{3+} complexes, the macrocycle twists around the metal to form a decadentate, helical binding pocket using both N_3O_2 binding motifs in the molecule (Fig. 5b). The two macrocycles crystallise as stacked pairs within the asymmetric unit with a Eu^{3+}–Eu^{3+} distance of 6.48 Å. The two complexes are very similar, both adopting the same helical form (*P*-shown in Fig. 5b); while they are chemically identical, they are crystallographically unique. Since the space group has inversion symmetry the crystal contains a racemic mixture. The two N_3O_2 binding motifs are arranged at ~62° with respect to each other, deviating from the orthogonality observed in non-macrocyclic 2 : 1 complexes.[12] This difference is probably due to the steric constraints imposed by the macrocyclic backbone.

The solution studies discussed above suggested that upon metal complexation **1** would undergo a significant conformational change with, as expected, the acyl-hydrazone moieties

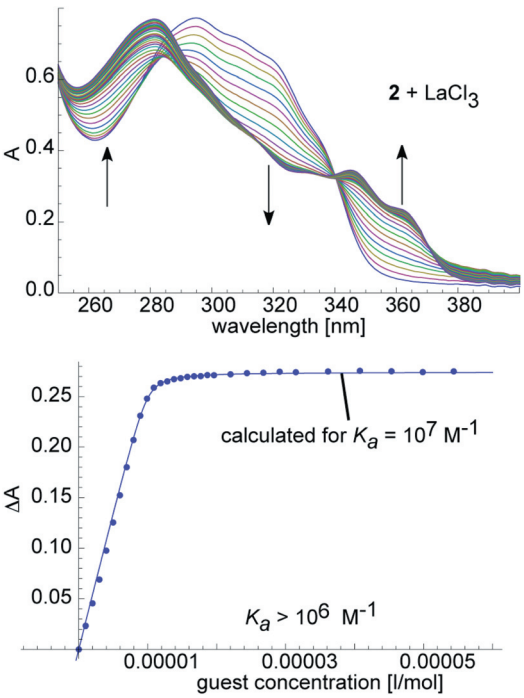

Fig. 3 UV-Vis spectra of **2** with different amounts of $LaCl_3$ (top, changes in the spectra are indicated by arrows) and resulting binding isotherm (below). Changes in the absorption at 320 nm (dots) were plotted against guest concentration and fitted to a model for 1 : 1 binding (line). Plotting other wavelengths (360, 340, 300 nm) produced similar results. We attribute the lack of an isosbestic point at 280 nm to the excess of metal salt. 1 : 1 binding is consistent with the HRMS and NMR studies.

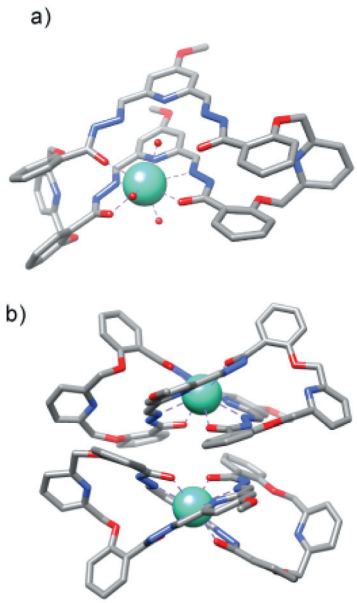

Fig. 5 (a) Schematic representation of the 9-coordinate complex in the structure of $[Eu(\mathbf{1})]_2[Eu(\mathbf{1})(H_2O)]\cdot 14H_2O\cdot 9Cl$ and (b) of the 10-coordinate complexes.

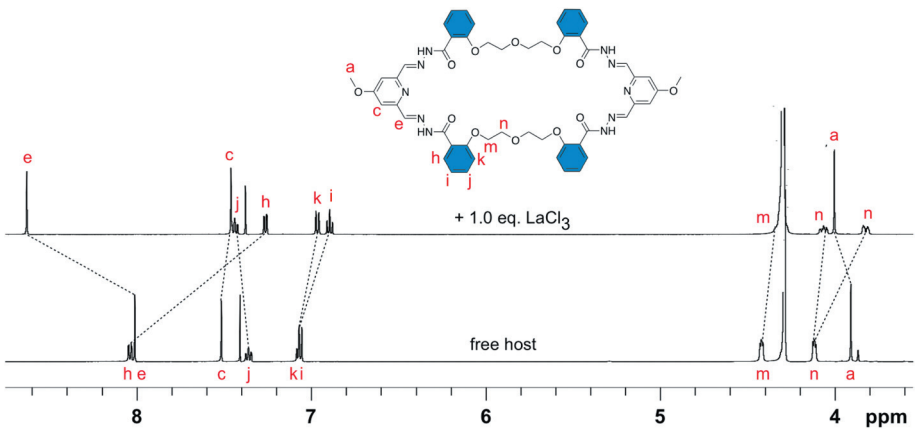

Fig. 4 ^1H NMR spectra (500 MHz, 297 K, $CDCl_3$–MeOD, 7 : 3) of **2** and its $LaCl_3$ complex.

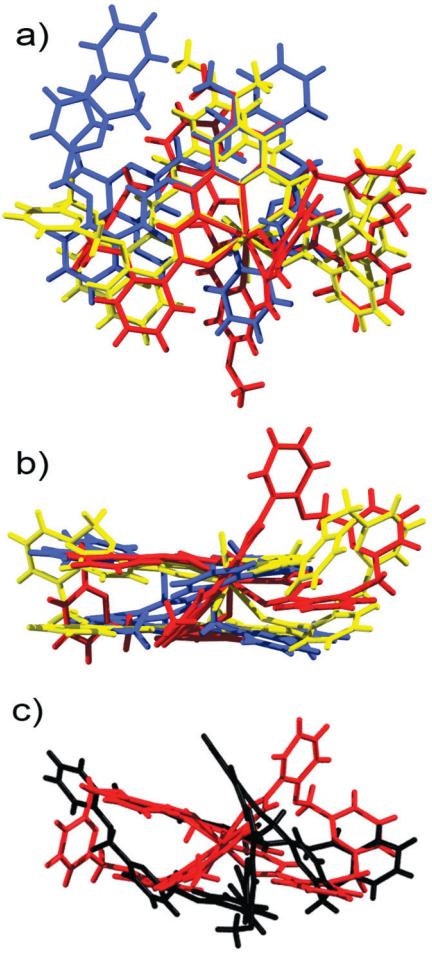

Fig. 6 (a) Top and (b) side view of an overlay of the crystal structures of $[Eu(\mathbf{1})]_2[Eu(\mathbf{1})(H_2O)]\cdot 14H_2O\cdot 9Cl$ and **1**·2MeOH; blue free ligand, red ten-coordinate complex, yellow nine-coordinate complex and (c) overlay of the ten-coordinate complex of $[Eu(\mathbf{1})]_2[Eu(\mathbf{1})(H_2O)]\cdot 14H_2O\cdot 9Cl$ (red) with the free ligand[7] from $\mathbf{1}\cdot 1.5\cdot H_2O\cdot 4CHCl_3$ (black).

reorientating from an 'open' to a 'closed' arrangement, allowing the hydrazone, pyridine and amide carbonyl to coordinate to the metal ion. Comparison of the nine-coordinate Eu^{3+} with the structure of **1**·2MeOH reveals some similarities in the overall structure of the macrocycle (Fig. 6): the two coordinating planes of the molecule are approximately the same distance apart as they are in the free ligand, while the S-shape of the macrocycle has not been retained. The most dramatic contrast is observed when comparing the structure of the ten-coordinate complex with the free ligand (Fig. 6). The helical complex, while having a close match in shape with the coordinating moieties of the flatter nine-coordinate species, otherwise does not have many conformational similarities with the rest of the nine-coordinate macrocycle or the free ligand. The conformation of the ten-coordinate complex is very similar to the twisted chiral arrangement observed in $\mathbf{1}\cdot 1.5H_2O\cdot 4CHCl_3$[7] (Fig. 6c) suggesting crystal packing (including solvation) effects can have a significant effect on the solid state conformation.

Crystals of $[La(\mathbf{2})(Cl)]\cdot 2Cl\cdot 1.75MeOH\cdot 7.35H_2O$ suitable for diffraction studies were obtained by the slow evaporation of a MeOH–H_2O solution. The lanthanide centre is eleven

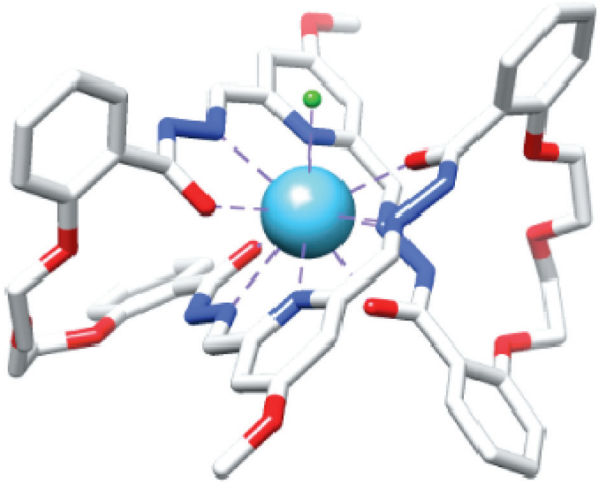

Fig. 7 Schematic representation of the X-ray structure of $[La(\mathbf{2})(Cl)]\cdot 2Cl\cdot 1.75MeOH\cdot 7.35H_2O$.

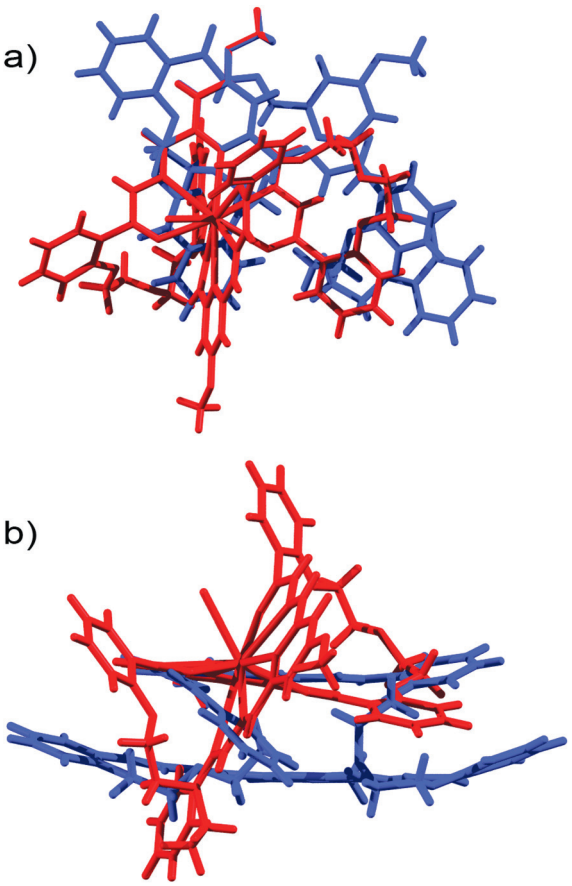

Fig. 8 (a) Overlay of the crystal structures of $[La(\mathbf{2})(Cl)]\cdot 2Cl\cdot 1.75MeOH\cdot 7.35H_2O$ (red) and **2**·MeOH[8] (blue) and (b) the same structures rotated approximately 90°.

coordinate, chelated to both of the acyl-hydrazone moieties in the macrocycle with the remaining site filled by a chloride anion, yielding an overall N_6O_4Cl-coordination sphere (Fig. 7). The two N_3O_2-binding groups are planar and arranged in a somewhat similar manner to those in the ten-coordinate europium complex

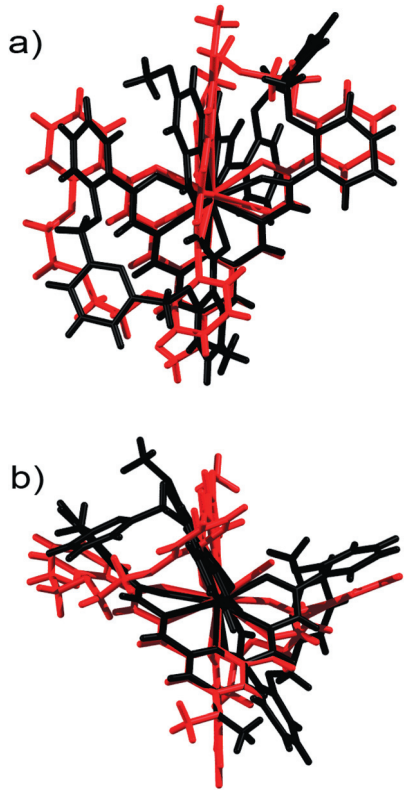

Fig. 9 (a) Overlay of $[La(\mathbf{2})(Cl)]^{2+}$ (red) and $[Eu(\mathbf{1})]^{3+}$ (black) and (b) the same structures rotated approximately 90°.

of **1** discussed above, such that the macrocycle is twisted around the metal in a helical arrangement, with an angle of ~75° between the chelating planes. The crystal consists of a racemic mixture of both the *P* and *M* helical forms. The twisted form of the macrocycle is stabilised by intramolecular hydrogen bonds between two of the amide protons and the ethylene–glycol linking units. The two other amide protons are involved in intermolecular hydrogen bonds with both chloride anions and solvent water molecules. Further hydrogen bonding between solvents and anions leads to the formation of infinite 1D ribbon-like polymers of complexes that extend parallel to the crystallographic *a*-axis. Adjacent ribbons interact *via* offset face-to-face π–π stacking between salicylaldehyde-phenyl rings resulting in a two-dimensional sheet-like motif.

As was observed in the case of **1**, **2** is also expected to have undergone a significant conformational change upon binding the metal ion despite the similarities in the 2D NOESY spectra. As expected, all of the hydrazone moieties in the complex adopt a 'closed' arrangement although three were 'open' in the structure of **2**·MeOH.[8] Once again, the twisted shape of the ligand backbone contrasts strongly with the far more planar arrangement observed in **2**·MeOH, resulting in little overlap between their conformations (Fig. 8), indicating that regardless of the choice of linker employed, a helical conformation is preferred in the solid state. These arrangements represent a significant change in the folding of the macrocycles compared to the methanol solvated crystal structures of the free ligands.

The similarities between the complexes of **1** and **2** are more extensive. As mentioned above, in both cases the macrocycles wrap around the metal centres forming chiral helical arrangements with the angle between the chelate planes deviating significantly from orthogonality. While $[La(\mathbf{2})(Cl)]^{2+}$ is eleven-coordinate and $[Eu(\mathbf{1})]^{3+}$ is ten-coordinate there is close similarity between their structures (Fig. 9) with minor differences accounted for by contrasting coordination number and flexibility of linking groups.

Conclusions

Two 44-membered macrocycles and their complexes with La^{3+}, Eu^{3+} and Dy^{3+} have been prepared. The complexes were analysed in solution and two complexes have been characterised crystallographically along with the structure of the free host **1**·MeOH. Upon complexation the macrocycles undergo significant changes in conformation as observed both in solution and the solid state.

Acknowledgements

We thank the Marie-Curie Research Training Network (MRTN-CT-2006-035614, J.M.K., V.S., U.L., J.K.M.S.), the Marie Curie IIF scheme of the 7th EU Framework Program (J.K. C.) for funding and Dr John Davies for recording X-ray data.

Notes and references

1 J.-C. G. Bünzli and C. Piguet, *Chem. Soc. Rev.*, 2005, **34**, 1048–1077; C. Benelli and D. Gatteschi, *Chem. Rev.*, 2002, **102**, 2369–2388; Q. Zhou, P. J. Saines, N. Sharma, J. Ting, B. J. Kennedy, Z. Zhang, R. L. Withers and K. S. Wallwork, *Chem. Mater.*, 2008, **20**, 6666–6676; L. F. Lindoy and W. E. Moody, *J. Am. Chem. Soc.*, 1977, **99**, 5863–5870; L. F. Lindoy and W. E. Moody, *J. Am. Chem. Soc.*, 1975, **97**, 2275–2276; L. F. Lindoy and H. W. Louie, *J. Am. Chem. Soc.*, 1979, **101**, 841–847; E. L. Crossley, J. B. Aitken, S. Vogt, H. H. Harris and L. M. Rendina, *Angew. Chem., Int. Ed.*, 2010, **49**, 1231–1233; E. J. Werner, A. Datta, C. J. Jocher and K. N. Raymond, *Angew. Chem., Int. Ed.*, 2008, **47**, 8568–8580; S. Petoud, G. Muller, E. G. Moore, J. Xu, J. Sokolnicki, J. P. Riehl, U. N. Le, S. M. Cohen and K. N. Raymond, *J. Am. Chem. Soc.*, 2007, **129**, 77–83; A. Datta and K. N. Raymond, *Acc. Chem. Res.*, 2009, **42**, 938–947; S. K. Langley, N. F. Chilton, B. Moubaraki, T. Hooper, E. K. Brechin, M. Evangelisti and K. S. Murray, *Chem. Sci.*, 2011, **2**, 1166–1169; C. Piguet, J. C. G. Bunzli, G. Bernardinelli, G. Hopfgartner, S. Petoud and O. Schaad, *J. Am. Chem. Soc.*, 1996, **118**, 6681–6697; J.-C. G. Bünzli and C. Piguet, *Chem. Rev.*, 2002, **102**, 1897–1928.

2 J. C. G. Bünzli and G. R. Choppin, *Lanthanide Probes in Life, Chemical and Earth Sciences, Theory and Practice*, Elsevier, Amsterdam, 1989; M. Seitz, A. G. Oliver and K. N. Raymond, *J. Am. Chem. Soc.*, 2007, **129**, 11153–11160.

3 D. Parker and J. A. G. Williams, *J. Chem. Soc., Dalton Trans.*, 1996, 3613–3628; V. Alexander, *Chem. Rev.*, 1995, **95**, 273–342.

4 L. F. Lindoy, *The Chemistry of Macrocyclic Ligand Complexes*, Cambridge University Press, Cambridge, 1989.

5 M. Wenzel, K. Gloe, K. Gloe, G. Bernhard, J. K. Clegg, X.-K. Ji and L. F. Lindoy, *New J. Chem.*, 2008, **32**, 132–137; I. M. Vasilescu, D. J. Bray, J. K. Clegg, L. F. Lindoy, G. V. Meehan and G. Wei, *Dalton Trans.*, 2006, 5115–5117; V. Gasperov, K. Gloe, L. F. Lindoy and M. S. Mahinay, *Dalton Trans.*, 2004, 3829–3834; J. R. Price, M. Fainerman-Melnikova, R. R. Fenton, K. Gloe, L. F. Lindoy, T. Rambusch, B. W. Skelton, P. Turner, A. H. White and K. Wichmann, *Dalton Trans.*, 2004, 3715–3726; J. R. Price, J. K. Clegg, R. R. Fenton, L. F. Lindoy, J. C. McMurtrie, G. V. Meehan, A. Parkin, D. Perkins and P. Turner, *Aust. J. Chem.*, 2009, **62**, 1014–1019; J. K. Clegg, L. F. Lindoy, P. Thuery, Y. H. Lee, D. K. A. Kusumohastuti, C. Mora, H. H. Kim, J. H. Cho and Y. Kim, *J. Inclusion Phenom. Macrocyclic Chem.*, 2009, **65**, 49–57; I. M. Vasilescu, D. S. Baldwin, D. J. Bourne, J. K. Clegg, F. Li, L. F. Lindoy and G. V. Meehan, *Dalton Trans.*, 2011, **40**, 8675–8684.

6 P. T. Corbett, J. Leclaire, L. Vial, K. R. West, J.-L. Wietor, J. K. M. Sanders and S. Otto, *Chem. Rev.*, 2006, **106**, 3652–3711; S. R. Beeren and J. K. M. Sanders, in *Dynamic Combinatorial Chemistry*, ed. J. N. H. Reek and S. Otto, Wiley-VCH, Weinheim, 2010, pp. 1–22.

7 J. M. Klein, V. Saggiomo, L. Reck, M. McPartlin, G. D. Pantoş, U. Lüning and J. K. M. Sanders, *Chem. Commun.*, 2011, **47**, 3371–3373.

8 J. M. Klein, V. Saggiomo, L. Reck, U. Lüning and J. K. M. Sanders, *Org. Biomol. Chem.*, 2012, **10**, 60–66.

9 D. D. McRitchie, R. C. Palenik and G. J. Palenik, *Inorg. Chim. Acta*, 1976, **20**, L27–L28; C. Lorenzini, C. Pelizzi, G. Pelizzi and G. Predieri, *J. Chem. Soc., Dalton Trans.*, 1983, 721–727; J. Davis and G. J. Palenik, *Inorg. Chim. Acta*, 1985, **99**, L51–L52; A. E. Koziol, R. C. Palenik and G. J. Palenik, *Inorg. Chim. Acta*, 1986, **116**, L51–L51; A. Bonardi, C. Carini, C. Merlo, C. Pelizzi, G. Pelizzi, P. Tarasconi, F. Vitali and F. Cavatorta, *J. Chem. Soc., Dalton Trans.*, 1990, 2771–2777; R. Pedrido, M. J. Romero, M. R. Bermejo, A. M. Gonzalez-Noya, M. Maneiro, M. J. Rodriguez and G. Zaragoza, *Dalton Trans.*, 2006, 5304–5314.

10 J. E. Thomas, R. C. Palenik and G. J. Palenik, *Inorg. Chim. Acta*, 1979, **37**, L459–L460; J. E. Thomas and G. J. Palenik, *Inorg. Chim. Acta*, 1980, **44**, L303–L304; M. Albrecht, S. Mirtschin, O. Osetska, S. Dehn, D. Enders, R. Fröhlich, T. Pape and F. E. Hahn, *Eur. J. Inorg. Chem.*, 2007, 3276–3287; M. Albrecht, K. Witt and O. Blau, *J. Prakt. Chem.*, 1998, **340**, 562–566.

11 R. C. Palenik, K. A. Abboud, S. P. Summers, L. L. Reitfort and G. J. Palenik, *Inorg. Chim. Acta*, 2006, **359**, 4645–4650.

12 M. Albrecht, Y. Yulia, A. Exarchos, P. Nachev and R. Fröhlich, *Dalton Trans.*, 2009, 7421–7427.

13 COLLECT, Nonius BV, 1998.

14 Z. Otwinowski and W. Minor, *Methods Enzymol.*, 1997, **276**, 307–326.

15 L. Farrugia, *J. Appl. Crystallogr.*, 1999, **32**, 837–838.

16 A. Altomare, M. C. Burla, M. Camalli, G. Cascarano, C. Giacovazzo, A. Guagliardi and G. Polidori, *J. Appl. Crystallogr.*, 1994, **27**, 435.

17 L. Palatinus and G. Chapuis, *J. Appl. Crystallogr.*, 2007, **40**, 786–790.

18 R. H. Blessing, *Acta Crystallogr., Sect. A: Found. Crystallogr.*, 1995, **51**, 33–38.

19 G. M. Sheldrick, *SHELXL-97, Program for refinement of crystal structures*, University of Göttingen, Germany, 1997.

20 C. A. Hunter and J. K. M. Sanders, *J. Am. Chem. Soc.*, 1990, **112**, 5525–5534.

21 C. Pelizzi and G. Pelizzi, *Acta Crystallogr., Sect. B: Struct. Crystallogr. Cryst. Chem.*, 1979, **35**, 126–128; M. R. Bermejo, R. Pedrido, A. M. Gonzalez-Noya, M. J. Romero, M. Vazquez and L. Sorace, *New J. Chem.*, 2003, **27**, 1753–1759.

22 F. Dumitru, Y.-M. Legrand, M. Barboiu, E. Petit and A. v. d. Lee, *Cryst. Growth Des.*, 2009, **9**, 2917–2921.

23 Y. R. Hristova, M. M. J. Smulders, J. K. Clegg, B. Breiner and J. R. Nitschke, *Chem. Sci.*, 2011, **2**, 638–641.

